THE JOURNAL OF
PHYSICAL CHEMISTRY A

Subscriber access provided by GEORGIAN COURT UNIVERSITY

Article

Switching of the Triplet-Triplet-Annihilation Upconversion with Photoresponsive Triplet Energy Acceptor: Photocontrollable Singlet/Triplet Energy Transfer and Electron Transfer

Kejing Xu, Jianzhang Zhao, Xiaoneng Cui, and Jie Ma

J. Phys. Chem. A, **Just Accepted Manuscript** • DOI: 10.1021/jp5111828 • Publication Date (Web): 16 Dec 2014

Downloaded from http://pubs.acs.org on December 20, 2014

Just Accepted

“Just Accepted” manuscripts have been peer-reviewed and accepted for publication. They are posted online prior to technical editing, formatting for publication and author proofing. The American Chemical Society provides “Just Accepted” as a free service to the research community to expedite the dissemination of scientific material as soon as possible after acceptance. “Just Accepted” manuscripts appear in full in PDF format accompanied by an HTML abstract. “Just Accepted” manuscripts have been fully peer reviewed, but should not be considered the official version of record. They are accessible to all readers and citable by the Digital Object Identifier (DOI®). “Just Accepted” is an optional service offered to authors. Therefore, the “Just Accepted” Web site may not include all articles that will be published in the journal. After a manuscript is technically edited and formatted, it will be removed from the “Just Accepted” Web site and published as an ASAP article. Note that technical editing may introduce minor changes to the manuscript text and/or graphics which could affect content, and all legal disclaimers and ethical guidelines that apply to the journal pertain. ACS cannot be held responsible for errors or consequences arising from the use of information contained in these “Just Accepted” manuscripts.

ACS Publications
High quality. High impact.

The Journal of Physical Chemistry A is published by the American Chemical Society.
1155 Sixteenth Street N.W., Washington, DC 20036

Published by American Chemical Society. Copyright © American Chemical Society. However, no copyright claim is made to original U.S. Government works, or works produced by employees of any Commonwealth realm Crown government in the course of their duties.

Switching of the Triplet-Triplet-Annihilation Upconversion with Photoresponsive Triplet Energy Acceptor: Photocontrollable Singlet/Triplet Energy Transfer and Electron Transfer

Kejing Xu, Jianzhang Zhao Xiaoneng Cui and Jie Ma*

State Key Laboratory of Fine Chemicals, School of Chemical Engineering, Dalian University of Technology, Dalian 116024 (China)

E-mail: zhaojzh@dlut.edu.cn; Web: http://finechem2.dlut.edu.cn/photochem

Abstract: A photoswitchable fluorescent triad based on two 9,10-diphenylanthracene (**DPA**) and one dithienylethene (**DTE**) moiety is prepared for photoswitching of triplet-triplet annihilation upconversion. The **DPA** and **DTE** moieties in the triad were connected via Click reaction. The **DPA** unit in the triad was used as the triplet energy acceptor and upconverted fluorescence emitter. The fluorescence of the triad is switched ON with the **DTE** moiety in open form (**DTE-(o)**) (upconversion quantum yield Φ_{UC} = 1.2%). Upon UV irradiation, photocyclization of the **DTE-(o)** moiety produces the closed form (**DTE-(c)**), as a result the fluorescence of **DPA** moiety was switched off (Φ_{UC} is negligible). *Three* different mechanisms are responsible for the fluorescence photoswitching effect, i.e. the photoactivated fluorescence-resonance-energy-transfer (FRET), the *intramolecular* electron transfer, as well as the photoactivated *intermolecular* triplet energy transfer between the photosensitizer and **DTE-(c)** moiety. Previously the photoswitching of TTA upconversion was accomplished with only *one* mechanism, i.e. the triplet state quenching of the photosensitizer by **DTE-(c)** via either the intermolecular or intramolecular energy transfer. The photophysical processes involved in the photochromism and photoswitching of TTA upconversion were studied with steady state UV–vis absorption and fluorescence emission spectroscopies, nanosecond transient absorption spectroscopy, electrochemical characterization, and DFT/TDDFT calculations.

Keywords: Energy Transfer; Photosensitizer; Switch; Triplet-triplet annihilation; Upconversion

■ INTRODUCTION

Photon upconversion is important for luminescent bioimaging,[1,2] photovoltaics,[3–5] and photocatalytic hydrogen (H_2) production,[6] etc. Among the upconversion methods, triplet-triplet annihilation upconversion (TTA UC) has attracted much attention owing to the advantage of low power and non-coherent excitation requirement (less than 100 mW cm^{-2}, solar light is sufficient), strong absorption of the excitation energy, and high upconversion quantum yields.[7–10] However, the known TTA upconversion is uncontrollable via external stimuli, such as pH, light irradiation, or with chemical species.

On the other hand, dithienylethene (DTE) is a versatile photochromic chromophore.[11-29] Previously the fluorescence of Bodipy and other fluorophores were photoswitched by the appended DTE unit, via the mechanisms of fluorescence-resonance-energy-transfer (FRET),[30–34] or aggregation,[35] photoswitched electron transfer,[36–42] or disruption of π-conjugation framework.[11,43] For example, DTE-o gives absorption only in UV spectral region, whereas DTE-c normally gives absorption at ca. 600 nm.[11] Thus the fluorescence emission of the covalently attached fluorophore (which gives emission length shorter than ca. 600 nm) can be quenched by FRET.[44,45] Photoswitching of triplet state of transition metal complexes was also reported.[46–49] Since fluorescent compounds are used in TTA upconversion as triplet acceptor/upconverted fluorescence emitter,[8] we envisaged that a triplet acceptor/emitter in TTA upconversion, such as **DPA**, covalently linked with **DTE** chromophore, can be used as photoresponsive triplet acceptor/emitter for photoswitching of TTA upconversion. Such investigation will present a new strategy for photoswitching of TTA UC.

Recently we performed photoswitched TTA upconversion with dithienylethene (**DTE**) photochromic unit as intermolecular triplet energy quencher.[50] Such switchable TTA upconversion will offer unprecedented modulability for the application of TTA UC, for example, in photo-activatable localization microscopy (PALM), a popular super-resolution fluorescence microscopy.[51,52] It will be also significant for construction of molecular devices, and for study of photophysics of organic chromophores.[53]

Our previous approach is based on the mechanism of intermolecular triplet state quenching within the three-component mixture. The DTE compound shows switchable T_1 state energy level, thus in the closed form, the DTE compound acted as triplet energy acceptor to quench the triplet excited state of the photosensitizers, thus the TTA UC is switched off. Note the photocycloreversion DTE-(c)→DTE-(o) is usually non-efficient, otherwise the quenching effect of DTE-o will not last long. In the open form, the DTE moiety is with much higher T_1 state energy level, and the triplet state of the photosensitizer is unable to be quenched by DTE-o.[50] Thus photoswitchable TTA upconversion was achieved. However, in order to make this photoswitchable TTA upconversion more efficient, new photoswitching motif is desired.

Following this line, herein we prepared a 9,10-diphenylanthracene (DPA) derived triplet acceptor/emitter with DTE unit attached (**DD-o**. Scheme 1). Triad **DD-o** contains two DPA moieties and one DTE moiety. The three chromophores are linked together by the feasible Click reaction. In the open form, **DD-o** is effective for TTA upconversion, with DPA unit as the triplet energy acceptor/emitter. By photoswitching the DTE moiety in **DD-o** to the closed form (DD-c), the fluorescence of the DPA moiety in **DD-(c)** is quenched by FRET, thus the TTA upconversion is photoswitched off. Thereafter the TTA upconversion can be photoswitched ON upon irradiation of the triplet acceptor at 580 nm. Moreover, we confirmed that the fluorescence of the **DPA** moiety is not only quenched by FRET, the photoinduced *intramolecular* electron transfer also contributes to quenching effect. Furthermore, *intermolecular* triplet state energy transfer from the triplet photosensitizer to the DTE-(c) unit is also responsible for the switching of TTA UC. Thus the present photoswitchable TTA UC motif is with triple-mechanism, i.e. the FRET, intramolecular electron transfer, and the intermolecular triplet energy transfer. The photophysical processes of the photoswitching system were studied with steady state UV−vis absorption and fluorescence emission spectroscopies, nanosecond transient absorption spectroscopy, electrochemical characterization (cyclic voltammetry) and DFT/TDDFT calculations.

■ RESULTS AND DISCUSSIONS

Design and Synthesis of the compounds. In order to photoswitch the fluorescence of DPA, the photochromic unit DTE was covalently linked with DPA. The feasible Click reaction was used to link the chromophores together. The fluorescence of DPA is at 400 nm.[8,54] DTE-(o) shows absorption only in UV region, but DTE-(c) shows absorptions at ca. 600 nm,[11] thus photoswitchable FRET from DPA moiety to DTE-(c) moiety is envisaged.[32,55,56] With the DTE moiety in the open form, the DPA unit is able to fluoresce, since the S_1 state of DTE-o is much

Scheme 1. Dithienylethene Derivative (DTE) and DPA Derivatives (DD-o) Used in the Photoswitching of TTA UC [a]

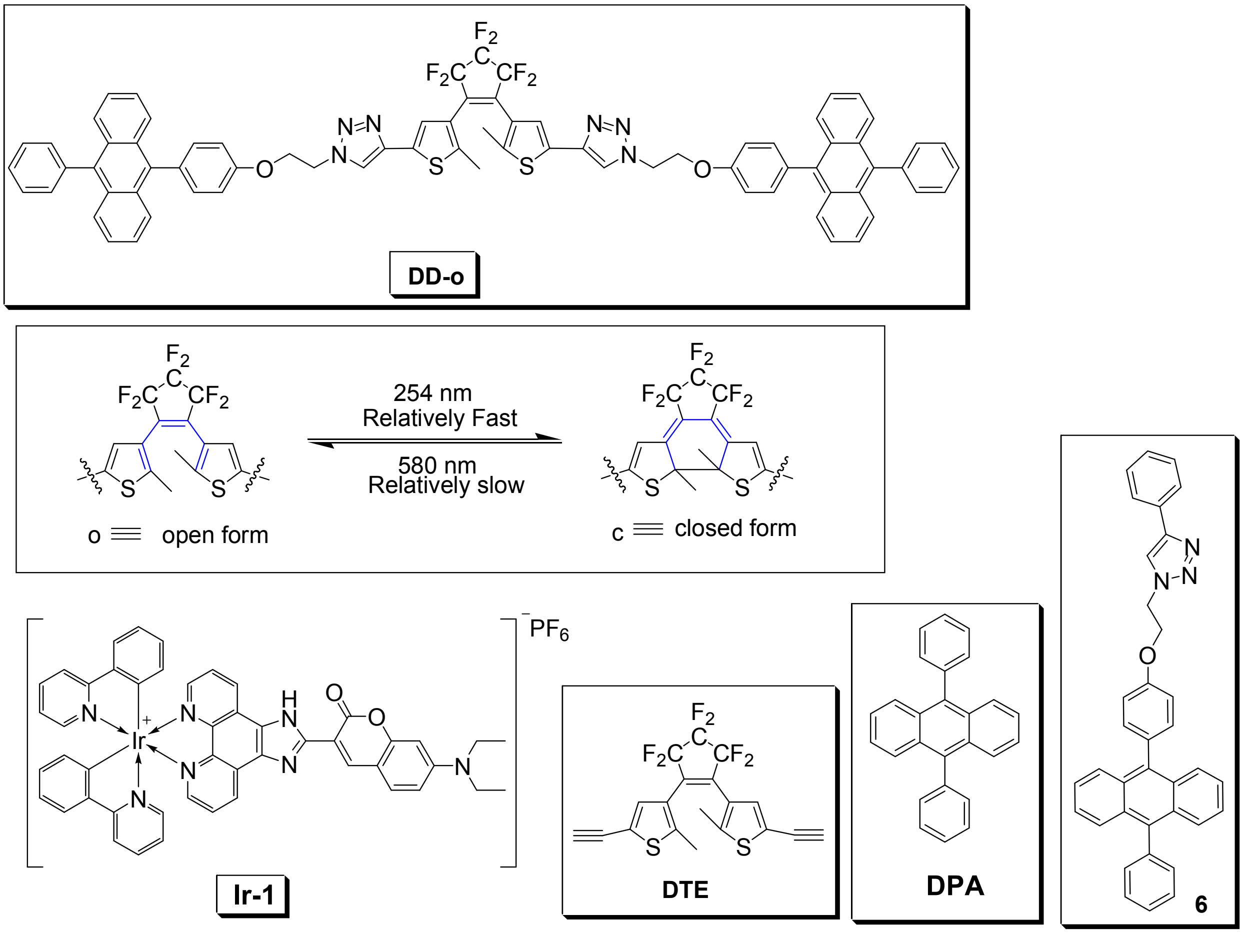

[a] **Ir-1** is the triplet photosensitizer and 9,10-Diphenylanthracene (DPA) is the triplet energy acceptor and emitter of the TTA upconversion.

Scheme 2. Synthesis of Compounds 1 – 5 and DD-o [a]

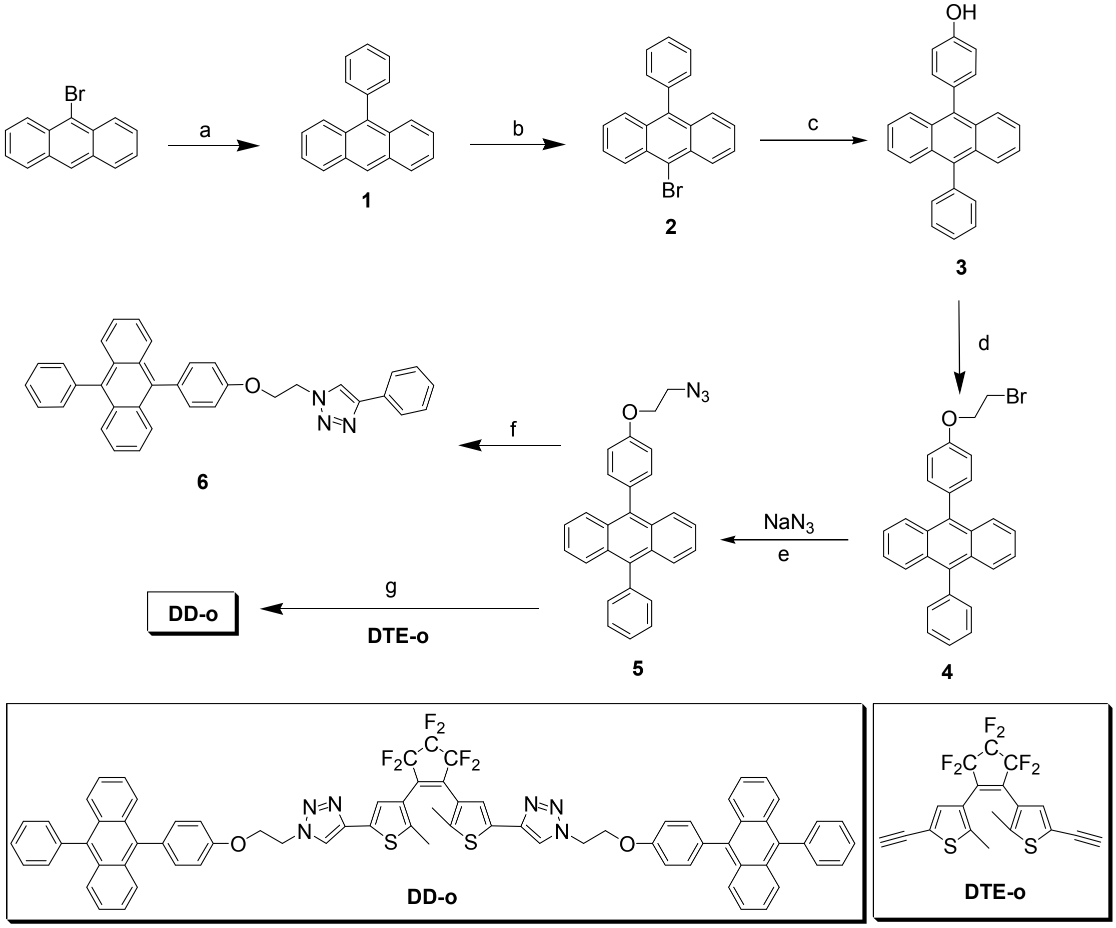

[a] Key: (a) Phenylboronic acid, K_2CO_3, $Pd(PPh_3)_4$, toluene/ ethanol/ water, reflux, 6 h. Yield: 93%; (b) Br_2, $CHCl_3$, r.t., 75 min. Yield: 82%; (c) 4-hydroxyphenylboronic acid, Na_2CO_3, $Pd(PPh_3)_4$, toluene/ ethanol/ water, reflux, 6 h. Yield: 69%; (d) 1,2-dibromoethane, anhydrous K_2CO_3, TBAB, dry acetone, reflux, 3d. Yield: 50%; (e) NaN_3, DMF, 100 °C, 1 h. Yield: 67%; (f) Phenylacetylene, Et_3N, $CuSO_4 \cdot 5H_2O$, and sodium ascorbate, 24 h, at r.t., in Ar, Yield: 71%; (g) similar with step f, Yield: 56%.

higher than the S_1 state of DPA moiety, thus no FRET exists to quench the fluorescence of DPA. Upon UV photoirradiation, DTE-o transformed into the closed form, DTE-c, for which the S_1 state energy level (approximated with the UV−vis absorption maximum) is lower than the S_1

state of DPA moiety, thus FRET will quench the fluorescence of **DPA** moiety. It should be pointed out that the photocycloreversion quantum yield of **DTE-c** is usually very low,[11] this property is crucial for **DTE-(c)** to be used as triplet state trap in the photoswitchable TTA upconversion, otherwise DTE-o will be produced and accumulated and the TTA upconversion OFF state will not last long. Thus the TTA upconversion can be photoswitched ON and OFF.[32] An Ir(III) complex **Ir-1** was used as the triplet photosensitizer due to its strong absorption of visible light and the long-lived triplet excited state.[57]

The synthesis of **DD-o** is with 9-bromoanthracene as starting material (Scheme 2). Suzuki cross coupling reaction with phenylboronic acid gives the product 9-bromo-10-phenylanthracene. A further Suzuki cross coupling reaction with 4-hydroxylphenylboronic acid gives the intermediate compound **3**. After two steps of routine synthesis, the azide compound **5** was obtained. The Cu(I)-catalyzed Click reaction between compound **5** and the ethynylated **DTE** compound **DTE-o** gives the target compound **DD-o**. All the compounds were obtained with moderate to satisfactory yields.

UV−vis absorption and fluorescence spectra. UV−vis absorption spectra of the compounds were studied (Figure 1). With the DTE unit in the open form, the major absorption of **DD-o** is attributed to the **DPA** moiety. Upon UV light irradiation (254 nm), a new broad absorption band centered at 580 nm was observed, which is due to the closed form of **DTE** moiety (**DD-c**). The absorption of **DD-o**/**DD-c** in the 350 nm – 450 nm is identical to that of **DPA**, thus we propose that there is no significant interaction between the chromophores in **DD** at the ground state.[32,58,59]

The fluorescence of **DD-o** and **DD-c** were compared with that of **DPA** (Figure 1b). The fluorescence of **DD-o** is close to that of **DPA**, whereas the fluorescence of **DD-c** is much weaker than **DPA** (quenched to 19.4% of the fluorescence intensity of **DD-(o)**). Based on the composition of the photostationary state (PSS. The **DD-(o)** is of 26.4% of the total **DD**), the fluorescence in **DD-c** is due to the residual **DD-o** in the PSS state.[32] The fluorescence of **DPA** moiety in the triad **DD** was significantly quenched in **DD-c**.[32,46,55]

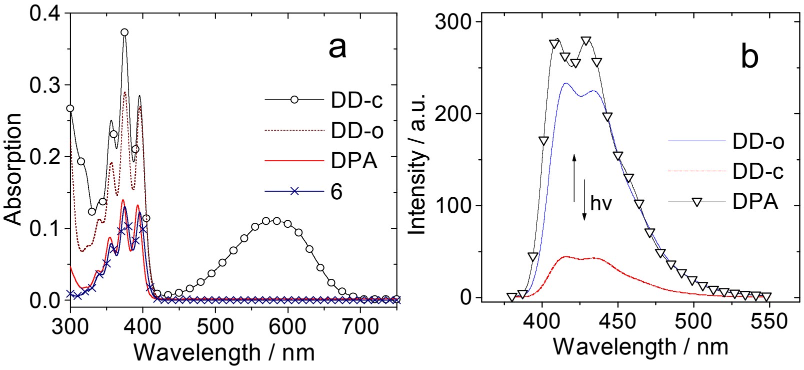

Figure 1. (a) UV−vis absorption spectra of **DD**, **DPA** and compound **6**. (b) The fluorescence emission spectrum of **DD-o**, **DD-c** and DPA, measured with optically matched solutions ($A_{372\text{ nm}}$ = 0.12). The concentration is slightly different. λ_{ex} = 372 nm. $c = 1.0 \times 10^{-5}$ M in toluene; 20°C.

The UV−vis absorption changes of **DD-o** during the photochromism were studied (Figure 2). Upon 254 nm irradiation of the **DD-o** solution, a new absorption band at 580 nm appeared (Figure 2a). This is due to the photocyclization of **DD-o** thus generation of **DD-c**. The process takes ca. 15 min to finish. The quantum yield of the photocyclization ($\Phi_{O\rightarrow C}$) was determined as 0.78% with chemical actinometer potassium ferrioxalate actinometer (see Supporting Information for details). The composition at the photostationary state (PSS) is with 26.4% of **DD-o** and 73.6% of **DD-c**. After establishment of the PSS with UV light, the solution was irradiated with 580 nm light, the absorption band at 580 nm decreased (Figure 2c). However, the photocycloreversion (**DD-c→DD-o**) process is much slower than the photocyclization (**DD-o→DD-c**). For the photocycloreversion, a very low quantum yield ($\Phi_{C\rightarrow O}$) of 0.02% was determined.[46,60] This non-efficient photocycloreversion is crucial for **DD-c** as the triplet/singlet energy trap for photoswitching of TTA UC (see later section for detail discussions). It should be noted that the quantum yields of the photocyclization and the photoreversion of DTE may vary substantially, depend on the molecular structures.[11,61] For example, previously the $\Phi_{O\rightarrow C}$ and $\Phi_{C\rightarrow O}$ of DTE-containing porphyrin derivatives were determined as 0.26% and 0.075%.[55] The color change of the solution accompanying the transformation is distinct. **DD-o** is almost colorless, whereas **DD-c** is in purple color (Figure 2a and 2b).

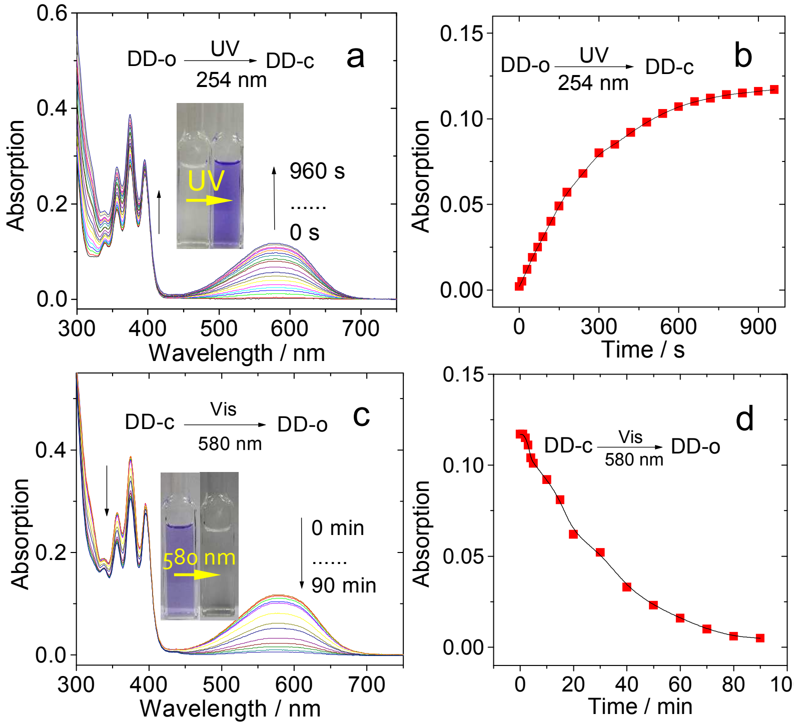

Figure 2. (a) Changes of UV–vis absorption spectra of **DD-o** upon irradiation with UV light (254 nm, 2.0 W/ m^2) and (b) the corresponding kinetics trace by following the absorption at 580 nm. (c) Changes of UV–vis absorption spectrum of **DD-c** upon visible light irradiation at 580 nm (10.0 W/ m^2) and (d) the corresponding kinetics trace by following the absorption at 580 nm. $c = 1 \times 10^{-5}$ M in toluene. Inset: the photographs of the solution taken at 1.0×10^{-4} M; 20 °C.

Photoswitching of the fluorescence of **DD-o** upon irradiation at 254 nm and 580 nm were also studied (Figure 3). For **DD-o**, strong blue fluorescence was observed (Φ_F = 82.9%). Upon 254 nm irradiation, the fluorescence intensity decreased (Figure 3a). At the PSS, the fluorescence

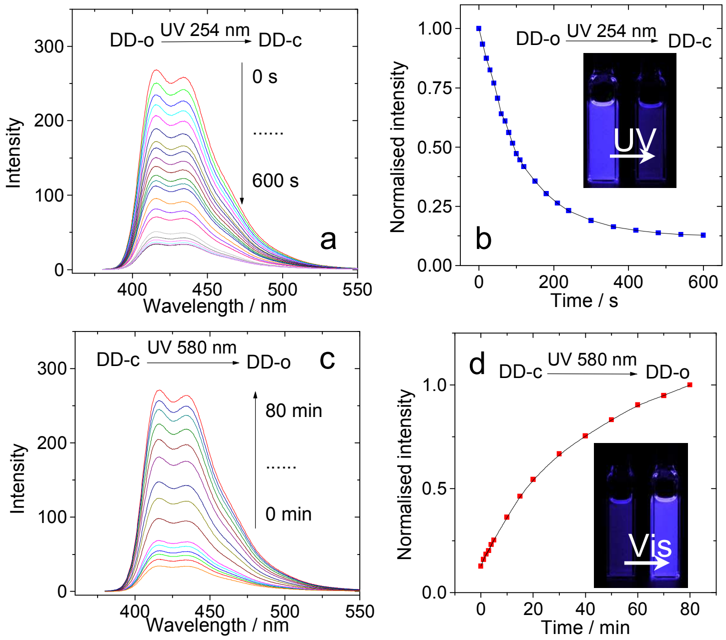

Figure 3. (a) Changes of fluorescence emission spectrum of **DD-o** upon irradiation with UV light (254 nm, 2.0 W/ m^2) and (b) the corresponding kinetic trace by monitoring the emission intensity at 416 nm. Inset: the photographs of the photoswitching of the emission; (c) Changes of emission spectrum of **DD-o** upon irradiation with visible light (580 nm, 10.0 W/ m^2) and (d) the corresponding kinetic trace by monitoring the emission intensity at 416 nm. Inset: the photographs of the photoswitched emission. λ_{ex} = 372 nm, $c = 1 \times 10^{-5}$ M, in aerated toluene; 20 °C.

was decreased to 12.8% of the original value (Φ_F = 17.1%). At PSS the fluorescence of **DD-c** was not completely switched off, which may be due to the equilibrium established at the PSS

(DD-o is of 26.4% of the PSS mixture).[39,46,47,55,62] The emission color of the **DD-o** faded from blue to dark (Figure 3b). The fluorescence recovery during the photocycloreversion upon 580 nm irradiation was also observed (Figure 3c). The fluorescence is nearly completely recovered. Correspondingly the emission of the solution was enhanced (Figure 3d). It is noticeable that the photoreversion is much slower than the photocyclization process (Figure 3b and 3d).

The reversibility, or the fatigue resistance of the system was studied with the UV−vis absorption and fluorescence responses (Figure S17, Supporting Information). The results show that the switching of UV−vis absorption and the fluorescence is reversible, no significant loss of the fluorescence intensity was observed after three cycles. It is known that DTE is resistant to photodecomposition. Furthermore, we found that the photocyclization quantum yield in toluene is much lower than that in dichloromethane and acetonitrile.[46]

Table 1. Photophysical Parameters of the Compounds [a]

	λ_{abs}/nm	ε [b]	λ_{em}/nm	τ_F /ns [c]	Φ_F (%) [d]	$\Phi_{O\rightarrow C}$ (%) [e]	$\Phi_{C\rightarrow O}$ (%) [f]
Ir-1	436	5.3	489	3.35	0.7	–[g]	–[g]
DD-o	375	2.9	416	4.40	82.9	0.78	–[g]
DD-c	375/ 580	3.7/ 1.1	416	4.52	17.1[h]	–[g]	0.015
DTE-o	282	2.2	–[g]	–[g]	–[g]	0.68	–[g]
DTE-c	570	0.75	–[g]	–[g]	–[g]	–[g]	0.084
DPA	373	1.4	408	5.30	92.5	–[g]	–[g]
6	375	1.3	416	4.83	86.3	–[g]	–[g]

[a] In toluene, c =1.0 × 10^{-5} M. [b] Molar absorption coefficient. ε : 10^{4} M^{-1} cm^{-1}. [c] Fluorescence lifetimes. [d] Fluorescence quantum yields, determined with 9,10-diphenylanthracene (DPA) as reference (Φ_F = 95.0 % in cyclohexane). [e] The quantum yields of the photochromism of $DTE_{O\rightarrow C}$ and $DD_{O\rightarrow C}$. [f] The quantum yields of the photochromism of $DTE_{C\rightarrow O}$ and $DD_{C\rightarrow O}$. [g] Not applicable. [h] Determined at the photostationary state (PSS).

The photophysical properties of the compounds were summarized in Table 1. The fluorescence quantum yield of **DD-o** (Φ_F = 82.9%) is slightly decreased as compared with that of **DPA** (Φ_F = 92.5%). Upon photocyclization, the **DD-c** shows much smaller fluorescence quantum yield (Φ_F =17.1%). Thus the photoswitching effect is significant.

Fluorescence Quenching Mechanism. We have shown that the fluorescence of **DD-o** is switched off by the photocyclization of **DTE** moiety (Figure 3a). In order to study the quenching mechanism, the fluorescence lifetimes of the compounds were determined with the time correlated single photon counting technique (TCSPC) (Figure 4). It is known that kinetic quenching will give reduced fluorescence lifetimes, whereas the static quenching of fluorescence does not show any fluorescence lifetime changes.[63] **DPA** gives fluorescence lifetime of 5.30 ns. **DD-o** give slightly shorter fluorescence lifetime of 4.40 ns.

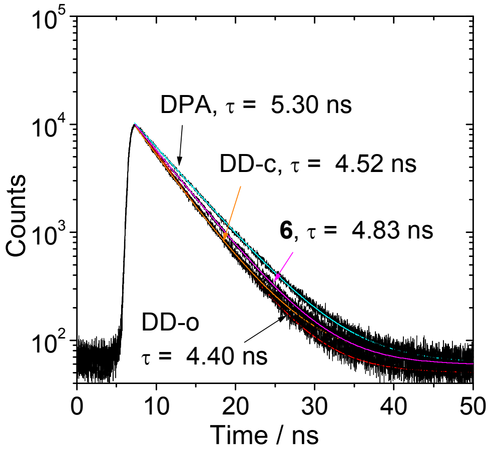

Figure 4. The fluorescence lifetime curves of **DD-o**, **DD-c** and compound **6** by monitoring the emission at 416 nm. Excited at λ_{ex} = 405 nm (picosecond pulsed laser), $c = 1.0 \times 10^{-5}$ M in toluene; 20 °C.

Note the fluorescence quantum yield **DD-(o)** (Φ_F = 82.9%) is close to **DPA** (Φ_F = 92.5%) and compound **6** (Φ_F = 86.3%). Interestingly, **DD-c** gives fluorescence lifetime of 4.52 ns, but the fluorescence quantum yield was greatly reduced (Φ_F =17.1%, Table 1, at PSS). Considering the determination error, we can consider that the fluorescence lifetime of **DD-o** and **DD-c** are very close. Note that the fluorescence of **DD-c** is much weaker than that of **DD-o**. Thus we propose the quenching of the fluorescence in **DD-c** (at PSS) is similar to a static quenching,[63] that is, for the molecules with DTE unit in closed form, the fluorescence of the DPA unit is completely quenched and this portion does not contribute to the lifetime value; the fluorescence of **DD-c** (at PSS) is from the residual **DD-o** species in the PSS mixtures of the closed and opened isomers.

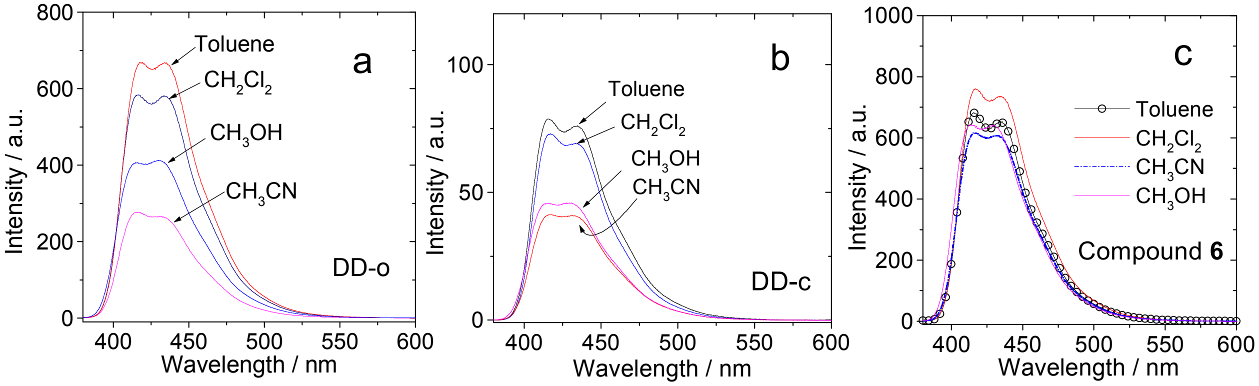

Figure 5. Fluorescence emission spectra of (a) **DD-o**, (b) **DD-c** and (c) compound **6** in solvents with different polarity. λ_{ex} = 372 nm, c = 1.0 × 10^{-5} M; 20 °C.

Besides the FRET, other photophysical processes may also contribute to the quenching of the fluorescence of a multichromophore molecular assembly, such as photoinduced electron transfer (PET). In order to study the PET effect, the fluorescence emission spectra of **DD-o** in solvents with different polarity were compared with that of compound **6**, which contains only the **DPA** moiety (Figure 5). The fluorescence emission intensity of compound **6** is almost independent on the solvent polarity, for that similar fluorescence emission intensity was observed in solvents of toluene, dichloromethane, acetonitrile and methanol (Figure 5c). For **DD-o** and **DD-c**, however, the fluorescence emission intensity was quenched by half in acetonitrile than that in toluene (Figure 5a and 5b). Note that the emission wavelength in toluene and acetonitrile are similar, thus the quenching is due to intramolecular charge transfer.[30,63] The UV−vis absorption spectra did not show such significant variation in different solvents (Figure S21, Supporting Information).

Electrochemical Study: Cyclic Voltammetry. In order to study the photoinduced electron transfer in **DD-o** and **DD-c**, the redox property of the compounds were studied with cyclic voltammetry (Figure 6). The reference compounds were also studied. DPA shows reversible oxidation wave at +0.87 V, and reversible reduction wave at −2.31 V was observed (Figure 6a). For compounds **6**, similar redox potentials were observed (Figure 6b). For **DD-o**, besides the redox waves assigned to the DPA moieties, an irreversible reduction wave at −1.89 V was found

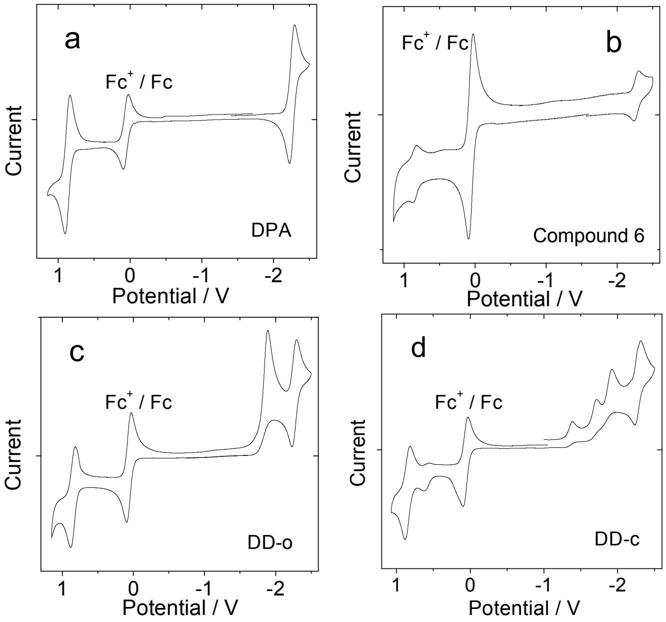

Figure 6. Cyclic voltammogram of (a) DPA, (b) compound **6**, (c) **DD-o** and (d) **DD-c**. In deaerated CH_3CN containing 0.10 M Bu_4NPF_6 as supporting electrode, $Ag/AgNO_3$ reference electrode. Scan rates: 50 mV/s. Ferrocene (Fc) was used as internal reference. $c = 1.0 \times 10^{-3}$ M, 20 °C.

(Figure 6c). For the **DD-c**, an pseudo-reversible oxidation wave at +0.59 V was observed. A few irreversible reduction waves at −1.39 V, −1.72 V and −2.27 V were observed (Figure 6d).

In order to study the photo-induced electron transfer in **DD-o** and **DD-c**, the Gibbs free energy changes (ΔG_{CS}) of the electron transfer processes were calculated with the Rohm-Weller equation (eq. 1 and eq. 2. See the Supporting Information for the detail procedure of the calculations),[59]

$$\Delta G^{0}{}_{\mathrm{CS}} = e[E_{OX} - E_{RED}] - E_{00} + \Delta G_{\mathrm{S}} \qquad \text{(Eq. 1)}$$

$$\Delta G_{\mathrm{S}} = -\frac{e^2}{4\pi\varepsilon_{\mathrm{S}}\varepsilon_0 R_{\mathrm{CC}}} - \frac{e^2}{8\pi\varepsilon_0}\left(\frac{1}{R_D} + \frac{1}{R_{\mathrm{A}}}\right)\left(\frac{1}{\varepsilon_{REF}} - \frac{1}{\varepsilon_S}\right) \qquad \text{(Eq. 2)}$$

Where ΔG_{S} is the static Coulombic energy, which is described by eq. 2. e = electronic charge, E_{OX} = half-wave potential for mono-electron oxidation of the electron-donor unit, E_{RED} = half-wave potential for one-electron reduction of the electron-acceptor unit; note herein the anodic and cathodic peak potentials were used because in some cases the oxidation is irreversible therefore the formal potential $E_{1/2}$ cannot be derived; E_{00} = energy level approximated with the fluorescence emission wavelength (for the singlet excited state). ε_{S} = static dielectric constant of the solvent, R_{CC} = (15.5 Å) center-to-center separation distance determined by DFT optimization of the geometry, R_{D} is the radius of the electron donor, R_{A} is the radius of the electron acceptor,

ε_{REF} is the static dielectric constant of the solvent used for the electrochemical studies, ε_0 permittivity of free space. The solvents used in the calculation of free energy of the electron transfer are CH_3CN ($\varepsilon = 37.5$), CH_2Cl_2 ($\varepsilon = 8.93$), toluene ($\varepsilon = 2.4$, 20 °C). The redox potentials and the free energy changes of the electron transfer were compiled in Table 2.

Table 2. Redox Potentials of DPA, Compound 6, DD-o and DD-c [a]

	E(ox) / V	E(red) / V
DPA	+ 0.87	– 2.31
Compound 6	+ 0.85	– 2.27
DD-o	+ 0.85	– 1.89, – 2.26
DD-c	+ 0.85, + 0.59	– 1.39, – 1.72, – 2.27

[a] Cyclic voltammetry in N_2 saturated CH_3CN containing a 0.10 M $BuNPF_6$ supporting electrolyte; Counter electrode is Pt electrode; working electrode is glassy carbon electrode; $Ag/AgNO_3$ couple as the reference electrode.

Table 3. The Data of Charge Separation (ΔG_{CS}) and Charge Separation Energy States (E_{CTS}) for DD-o and DD-c in Different Solution [a]

	ΔG_{CS} (eV)			E_{CTS} (eV)		
	Toluene	CH_2Cl_2	CH_3CN	Toluene	CH_2Cl_2	CH_3CN
$^1DPA^* \rightarrow$ DTE-o	+0.38	–0.12	– 0.26	+3.36	+2.86	+2.72
$^1DPA^* \rightarrow$ DTE-c	– 0.12	– 0.62	– 0.77	+2.86	+2.36	+2.21
DTE-c $\rightarrow$ $^1DPA^*$	+0.50	0.002	– 0.14	+3.48	+3.00	+2.84

[a] The arrow indicated the direction of electron transfer. "1 and *" means this part of the triad is at its singlet excited state.

The results show that for **DD-o** in toluene, the photoinduced intramolecular electron transfer is thermodynamically prohibited because the Gibbs free energy changes (ΔG_{CS}) is +0.38 eV. In polar solvents such as CH_2Cl_2 and CH_3CN, however, the values are –0.12 eV and –0.26 eV, thus

PET is a thermodynamically allowed process for **DD-o** in polar solvents. This conclusion is in agreement with the fluorescence emission of **DD-o** in solvents with different polarity (Figure 5), which show that the fluorescence of **DD-o** was quenched in polar solvents. Previously it was reported that the electron transfer in DTE-containing perylenebisimide (PBI) compounds and Ru(II) complex was modulated by the photocyclization and photoreversion of DTE.[36,41]

The Gibbs free energy changes of the possible PET in **DD-c** were also calculated. It was found that PET is possible even in toluene ($\Delta G_{\mathrm{CS}} = -0.12$ eV). The driving forces for PET in polar solvents such as CH_2Cl_2 and CH_3CN are larger. These data suggest that the fluorescence of **DD-c** may be drastically quenched in polar solvents, which is in agreement with the experimental results.

Photoswitching of the TTA Upconversion. The photoswitching of the TTA upconversion with **DD-o** as triplet acceptor/emitter was studied (Figure 7). An Ir(III) complex showing strong absorption of visible light-absorption and long-lived triplet excited state was used as triplet

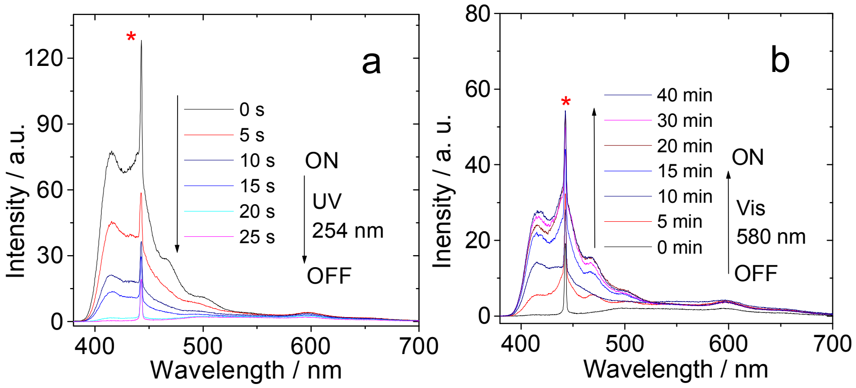

Figure 7. Photoswitching of the TTA upconversion with **Ir-1** as photosensitizer and **DD-o/c** as triplet energy acceptor. (a) The upconverted fluorescence with **DD-o** as triplet energy acceptor/emitter upon 254 nm photoirradiation (switching off of the upconversion); (b) The upconverted fluorescence with **DD-c** as triplet energy acceptor/emitter upon 580 nm

photoirradiation (switching off of the upconversion). Upconversion was performed upon excitation with a 445 nm continuous laser (power density is 5.0 mW). $c = 1.0 \times 10^{-5}$ M in toluene, 20 °C.

photosensitizer.[57] TTA upconversion was observed with **DD-o** as the triplet acceptor/emitter. Upon 254 nm irradiation, the upconversion emission intensity decreased, and was completely switched off after 25 s of UV irradiation (254 nm irradiation).

We found that the open form→closed form photocyclization is unable to be sensitized via intermolecular triplet energy transfer between **Ir-1** and **DD-o** (see the Supporting Information, Figure S19). Previously it was reported that the photocyclization of DTE was sensitized by intramolecular triplet energy transfer in Ru(II) or Os(III) complexes.[46–48,64,65] Furthermore, triplet photosensitizer **Ir-1** is stable under the continues photoirradiation with 445 nm laser (see Supporting Information, Figure S20).

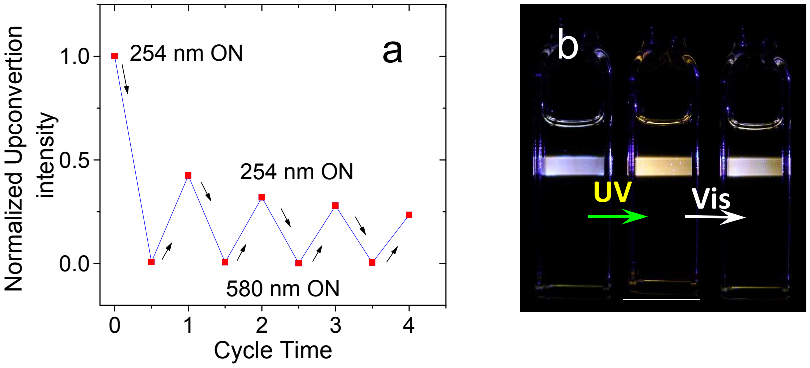

Figure 8. (a) The reversibility of the photoswitching of TTA upconversion with **DD-o/c** as photoactivatable triplet energy acceptor/emitter. (b) The photographs of the solutions in photoswitching of TTA upconversion. Upconversion was performed upon excitation with a 445 nm continuous laser (power density: 16.8 mW/ cm^2). $c = 1.0 \times 10^{-5}$ M in toluene; 20 °C.

Upon 580 nm photoirradiation, the TTA upconversion intensity recovered (Figure 7b). The switching process is reversible, although there is significant loss of the upconversion emission intensity after the first circle (Figure 8). This is due to the persistent presence of the **DD-c** in the mixture after the first time of UV irradiation (photocyclization).[66] Moreover, the switching OFF process of the TTA upconversion upon UV photoirradiation is much faster than recovery of the TTA upconversion upon visible light irradiation. This result indicates that the TTA upconversion is highly sensitive to the presence of the quencher (the DTE-c moiety). The photoswitching of the TTA upconversion is visible to unaided eye (Figure 8b). Thus these photocontrolable TTA upconversion may be used for photocontrollable luminescent bioimaging, or super-resolved fluorescence microscope (such as PALM), etc.[51]

In order to investigate the mechanism of the photoswitching of the TTA upconversion, the quenching of the triplet state of photosensitizer **Ir-1** were studied with the nanosecond transient absorption spectroscopy. Stern-Volmer quenching plots were constructed (Figure 9). The parent compound **DPA** was used as a benchmark.

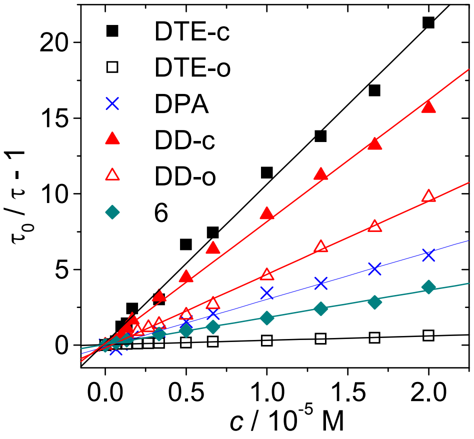

Figure 9. Stern−Volmer plots of the quenching of triplet state lifetime of **Ir-1** by **DTE-c**, **DTE-o**, **DD-c**, **DD-o**, **DPA** and compound **6**. The plots of **DTE-c** and **DD-c** were calculated according to

the open form/closed form ratio at the PSS. The triplet state lifetimes were determined with nanosecond transient absorption spectroscopy (λ_{ex} = 445 nm). c (**Ir-1**) = 1.0×10^{-5} M in deaerated toluene. 20 °C.

Compound **6** shows smaller quenching constant than that of **DPA**, this decreased quenching efficiency (i.e. the TTET efficiency) may be attributed to the large molecular size of compound **6** as compared with **DPA**. For **DD-o**, however, the quenching constant ($K_{SV} = 4.85 \times 10^5$ M^{-1}) is larger than DPA ($K_{SV} = 3.12 \times 10^5$ M^{-1}). This enhanced quenching effect with **DD-o** may be attributed to the dual **DPA** moieties in **DD-o**, which makes the quenching more efficient.

Table 4. Upconversion-related Parameters. Ir-1 as the Photosensitizer [a]

	DD-o	DD-c	DTE-c	DTE-o	6	DPA
Φ_{UC} (%) [b]	1.27	0.00	– [g]	– [g]	– [g]	19.7
K_{SV}/M^{-1} [10^5] [c]	4.85	8.04	10.48	0.29	1.79	3.12
k_q/M^{-1} s^{-1} [10^{10}] [d]	0.69	1.10	1.50	0.041	0.26	0.45
k_0/M^{-1} s^{-1} [10^{10}] [e]	1.11	1.12	1.69	1.57	1.20	1.50
f_Q [f]	0.62	1.00	0.89	0.03	0.21	0.30

[a] In deaerated toluene. [b] Upconversion quantum yields measured with **Ir-1** as the standard (Φ_P = 21.3 % in CH_3CN).[57] [c] Stern–Volmer quenching constants. [d] Bimolecular quenching constants. $K_{SV} = k_q\tau_0$, τ_0 = 70.0 μs. [e] Diffusion-controlled bimolecular quenching rating constants. [f] The quenching efficiency. [g] Not applicable.

For the **DD-c**, the quenching constant ($K_{SV} = 8.04 \times 10^5$ M^{-1}) is much larger than **DD-o** ($K_{SV} = 4.85 \times 10^5$ M^{-1}). This result indicate that the DTE-c moiety in DD-c is an extra triplet energy acceptor besides DPA moiety, i.e. the triplet state energy draining funnel, i.e. TTET, between the **Ir-1** and DTE-c moiety is activated. This enhanced quenching is supported with the parent DTE compounds, for which **DTE-c** gives much larger quenching constant ($K_{SV} = 1.05 \times 10^6$ M^{-1}) than the **DTE-o** ($K_{SV} = 2.9 \times 10^4$ M^{-1}). Thus, our quenching study shows that the TTET efficiency can be photoswitched by the DTE moiety. Larger triplet acceptor is disadvantageous as compared with that of smaller triplet acceptor concerning the diffusion-controlled bimolecular quenching constants, which are dependent on the molecular size. Previously DTE was used for photoactivated quenching of the triplet state of Zn(II)-porphyrin complex, but the quenching constant was not reported.[67]

In order to investigate the quenching efficiencies of the compounds, the diffusion-controlled bimolecular quenching constants were calculated with equation 3 (Table 4).[63]

$$k_0 = 4\pi RND/1000 = \frac{4\pi N}{1000}(R_f + R_q)(D_f + D_q) \qquad \text{(Eq. 3)}$$

D is the sum of the diffusion coefficients of the energy donor (D_f) and quencher (D_q), N is Avogadro's number. R is the collision radius, the sum of the molecule radii of the energy donor (R_f) and the quencher (R_q). Diffusion coefficients can be obtained from Stokes-Einstein equation:

$$D = k\mathrm{T} / 6\pi\eta R \qquad \text{(Eq. 4)}$$

k is Boltzmann's constant, η is the solvent viscosity, R is the molecule radius. The quenching efficiency f_Q can be obtained from eq.5:

$$f_Q = k_q / k_0 \qquad \text{(Eq. 5)}$$

Table 5. The Parameters Related to Calculation of the Quenching Efficiency f_Q [a]

	DD-o	**DD-c**	**DTE-c**	**DTE-o**	**6**	**DPA**
R_q/m $[10^{-10}]$	23.14	15.37	5.03	5.73	10.9	6.28
D_f/cm^{2}s^{-1}$[10^{-6}]$	1.86	1.86	1.86	1.86	1.86	1.86
D_q/cm^{2}s^{-1}$[10^{-6}]$	1.57	2.37	7.24	6.35	3.34	5.80

[a] In toluene, $\eta = 5.90 \times 10^{-4}$ Pa·s; $T = 293.15$ K; $R_f = 1.96 \times 10^{-9}$ m; D_f is the diffusion coefficients of the energy donor, D_q is the diffusion coefficients of the quencher.

The diffusion coefficients of DPA are larger than **DD-o** and **DD-c** (Table 5), due to the smaller molecular size of **DPA** than **DD-o** and **DD-c**. The diffusion-controlled bimolecular quenching constants of **DD-o** and **DD-c** are smaller than that of DPA (Table 4). However, the quenching efficiency of **DD-o** and **DD-c** are 2- and 3-fold of that of DPA. This result can be attributed to the two DPA units in **DD-o** and **DD-c**, thus the quenching chance per collision is higher for **DD-o** and **DD-c** than that of DPA.

DFT Calculations: the Excited State Energy Levels of the Triad. In order to study the photophysical properties of **DD-o** and **DD-c**, and the photoswitching of the TTA upconversion, DFT calculations were carried out. Firstly, the spin density surfaces of **DD-o** and **DD-c** were calculated (Figure 10). For **DD-o**, the spin density is confined on the DPA unit. For **DD-c**, however, the spin density surface is localized on the **DTE-c** moiety. This result is in agreement with the experimental observation (the triplet state quenching studies).

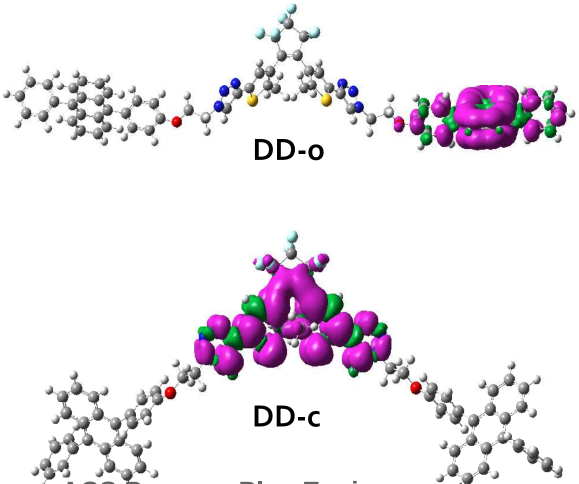

Figure 10. Isosurfaces of spin density of **DD-o** and **DD-c** at the optimized triplet state geometries. Calculation was performed at B3LYP/6-31G(d)/LANL2DZ level with Gaussian 09W.

The ground state geometry of **DD-o** was optimized, the excitation energy of the singlet excited states were calculated with the TDDFT methods (Figure 11 and Table 6). Two low-lying isoenergetic singlet excited states (S_1 and S_2 states) were obtained, which are confined on the two DPA units. The calculated excitation energy (3.09 eV, 400 nm) is in good agreement with the UV−vis absorption experimental results. The S_7 state is confined on the **DTE-o** unit, which

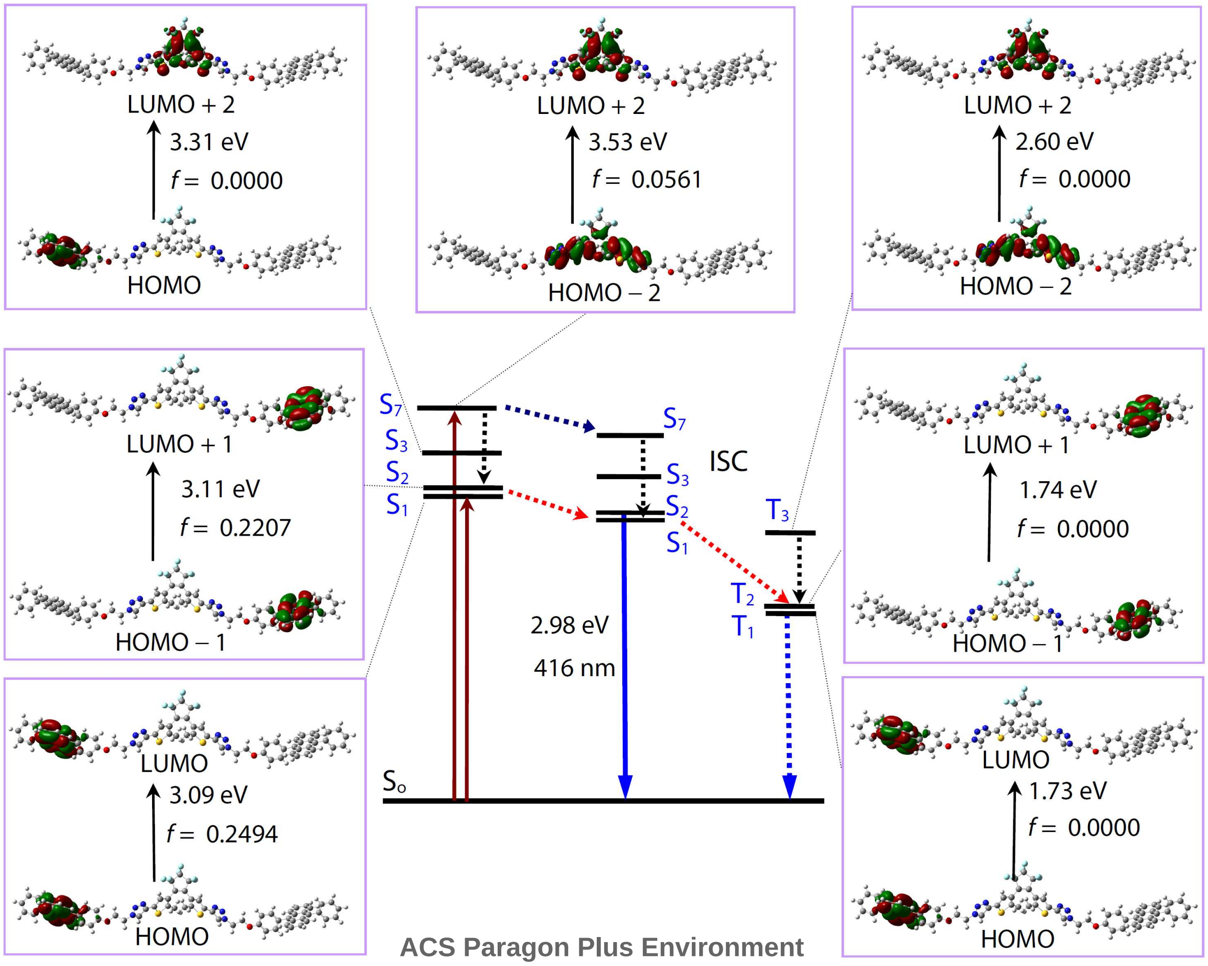

Figure 11. Selected frontier molecular orbitals involved in the singlet and triplet excited states of **DD-o**. The calculations were performed at the B3LYP/6-31G(d)/LANL2DZ level using Gaussian 09W. Toluene was used as solvent in the calculations.

is with much higher excitation energy (3.53 eV). Thus the order of the singlet excited state is in agreement with the experimental results.

The triplet state energy levels of **DD-o** were calculated with TDDFT method, based on the optimized ground state geometry. Two degenerated triplet states were obtained (T_1 and T_2 states), which are localized on the two DPA units in **DD-o**, respectively. The calculated energy levels (1.73 eV) are in agreement with the experimental results.[68] The T_3 state is localized on the **DTE-o** moiety, which is with much higher energy of 2.60 eV.

Table 6. Selected Parameters for the Vertical Excitation Energies (eV) (UV–vis absorption) and Oscillator Strengths (*f*), Configurations of the Low-Lying Excited States of DD-o. Calculated by TDDFT//B3LYP/6-31G(d)/LANL2DZ, Based on the Optimized Ground State Geometries (Toluene Was Used as Solvent in All the Calculations).

Electronic transition [a]		TDDFT/B3LYP/6-31G(d)			
		Excitation energy	f [b]	Composition [c]	CI [d]
Absorption	$S_0 \rightarrow S_1$	3.09 eV (400 nm)	0.2494	H→L	0.7018
	$S_0 \rightarrow S_2$	3.11 eV (398 nm)	0.2207	H–1→ L + 1	0.7019
	$S_0 \rightarrow S_7$	3.53 eV (351 nm)	0.0561	H–2 → L+ 2	0.6938
	$S_0 \rightarrow S_{29}$	4.35 eV (285 nm)	0.5317	H–2→ L+ 4	0.6773
Triplet states	$T_0 \rightarrow T_1$	1.73 eV (717 nm)	0.0000	H→ L	0.6984
	$T_0 \rightarrow T_2$	1.74 eV (715 nm)	0.0000	H–1→ L + 1	0.6997
	$T_0 \rightarrow T_3$	2.60 eV (478 nm)	0.0000	H–2→ L + 2	0.5536
	$T_0 \rightarrow T_4$	2.78 eV (447 nm)	0.0000	H–2→ L + 3	0.4827
	$T_0 \rightarrow T_5$	3.23 eV (384 nm)	0.0000	H–2→ L+ 4	0.4331

[a] Only selected excited states were considered. The numbers in parentheses are the excitation energy in wavelength. [b] Oscillator strength. [c] H stands for HOMO and L stands for LUMO. Only the main configurations are presented. [d] Coefficient of the wavefunction for each excitations. The CI coefficients are in absolute values. [e] Based on the optimized S_1 state geometry.

The excited states of **DD-c** were also studied with the TDDFT methods (Figure 12, Table 7). The calculated S_1 state is localized on DTE moiety, with excitation energy of 2.05 eV (604 nm). This calculated excitation energy is very close to the experimental results (absorption band of **DD-c** at 580 nm). The S_4 and S_5 states are localized on the two DPA moiety, respectively, which are with much higher excitation energy 3.10 eV. Thus FRET in **DD-c** is possible with DPA as the intramolecular singlet energy donor and the **DTE-c** moiety as the singlet energy acceptor.

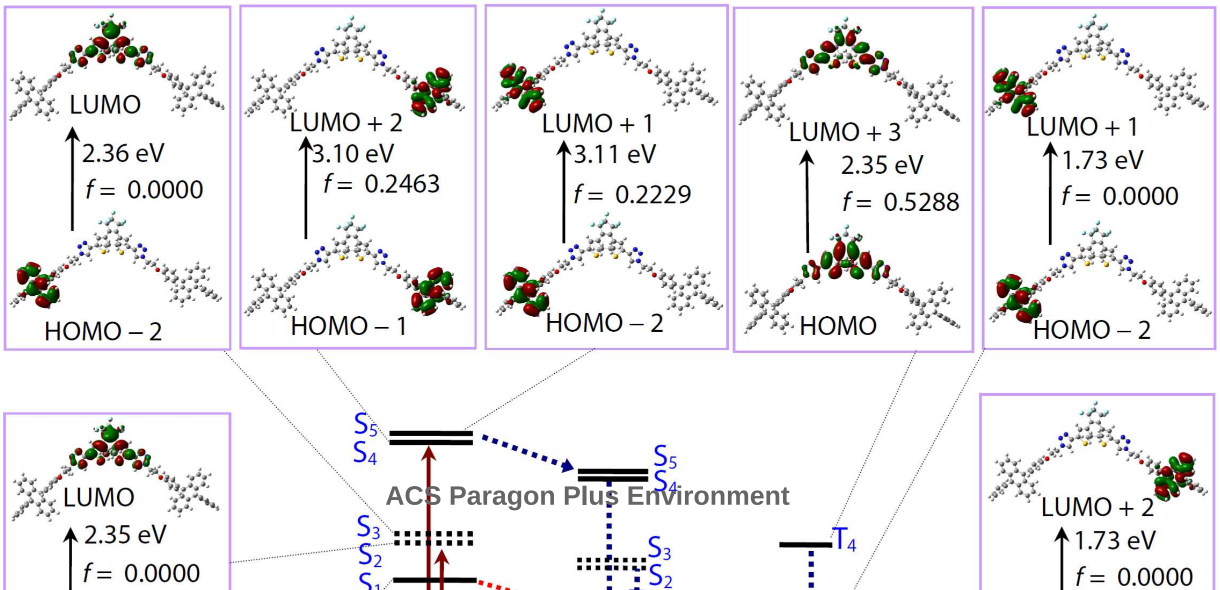

Figure 12. Selected frontier molecular orbitals involved in the excitation and emission of **DD-c** in toluene. The calculations are at the B3LYP/6-31G(d)/LANL2DZ level using Gaussian 09W.

The triplet state of **DD-c** was calculated. T_1 state is localized on the **DTE** moiety, with energy level of 0.96 eV. The triplet states localized on the two **DPA** moieties are with energy level of 1.73 eV, which is much higher than that of T_1 state. Thus the triplet state localized on the **DPA** moiety may be quenched by the intramolecular triplet energy transfer to the **DTE-c** moiety. This theoretical calculation results can be used for rationalization of the quenched TTA upconversion with the **DTE** moiety in the closed form.

Table 7. Selected parameters for the vertical excitation (UV-vis absorption), electronic excitation energies (eV) and oscillator strengths (*f*), configurations of the low-lying excited

states of DD-c. Calculated by TDDFT//B3LYP/6-31G(d)/LANL2DZ, based on the optimized ground state geometries (toluene was used as solvent in all the calculations)

Electronic transition [a]		TDDFT/B3LYP/6-31G(d)			
		Excitation energy	f [b]	Composition [c]	CI [d]
Absorption	$S_0 \rightarrow S_1$	2.05 eV (604 nm)	0.5288	H→L	0.7070
	$S_0 \rightarrow S_4$	3.10 eV (400 nm)	0.2463	H–1→ L + 2	0.7011
	$S_0 \rightarrow S_5$	3.11 eV (399 nm)	0.2229	H–2 → L+ 1	0.7009
	$S_0 \rightarrow S_{13}$	3.59 eV (345 nm)	0.1934	H→ L+ 3	0.5354
Triplet states	$T_0 \rightarrow T_1$	0.96 eV (1298 nm)	0.0000	H→ L	0.7169
	$T_0 \rightarrow T_2$	1.73 eV (716 nm)	0.0000	H–1→ L + 2	0.6988
	$T_0 \rightarrow T_3$	1.73 eV (715 nm)	0.0000	H–2→ L + 1	0.6995
	$T_0 \rightarrow T_4$	2.35 eV (527 nm)	0.0000	H→ L + 3	0.6739
	$T_0 \rightarrow T_5$	2.35 eV (526 nm)	0.0000	H–1→ L	0.6455

[a] Only selected excited states were considered. The numbers in parentheses are the excitation energy in wavelength. [b] Oscillator strength. [c] H stands for HOMO and L stands for LUMO. Only the main configurations are presented. [d] Coefficient of the wavefunction for each excitations. The CI coefficients are in absolute values. [e] Based on the optimized S_1 state geometry.

The photophysical processes involved in the **DD-o**, **DD-c** and the photoswitch of the TTA UC were summarized in Scheme 3. For **DD-o**, the S_1 state of the DTE-o moiety is higher in energy than the DPA moiety. Thus, no FRET exists to quench the fluorescence of DPA moiety. Moreover, the charge transfer state (CST) is with energy level of 3.35 eV, thus the fluorescence of DPA moiety is not perturbed by any electron transfer (in toluene). Therefore, **DD-o** shows similar fluorescence quantum yield as compared with that of DPA (Table 1). However, the energy level of CTS will decrease to 2.71 eV in polar solvents such as acetonitrile, as a result, the energy level is lower than the S_1 state energy level of the DPA moiety (2.98 eV), thus, fluorescence quenching of the DPA emission was observed in acetonitrile as compared to that in nonpolar solvent, such as toluene.

Scheme 3. Simplified Jablonski Diagram Illustrating the Photophysical Processes Involved in the Photoswitched TTA Upconversion, (a) DD-o as triplet acceptor/emitter, (b) DD-c as triplet acceptor/emitter [a]

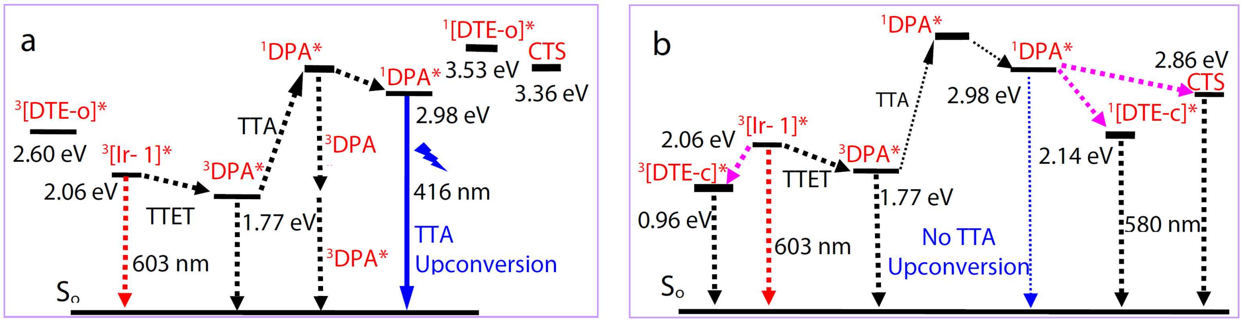

[a] The component at the excited state was designated with red color. The number of the superscript designated either the singlet or the triplet excited state. For clarity, the production of the triplet state of the Ir(III) complex by photoexcitation into the singlet excited state of the complex is omitted. The excitation of the **Ir-1** photosensitizer was omitted. Toluene as the solvent.

The DTE-o moiety is with T_1 state energy level of 2.60 eV, which is much higher than the DPA triplet state energy level (1.77 eV), therefore, the triplet state of DPA moiety is not quenched by DTE-o. Based on the above analysis, TTA upconversion should be observed with **DD-o**. It should be noted that the T_1 state of the photosensitizer (2.06 eV),[57] complex **Ir-1**, should not be quenched by DTE-o moiety either.

Upon UV irradiation, photocyclization of the DTE-o moiety will give **DD-c**, with the DTE moiety in closed form. Along with the photocyclization, the singlet excited state energy level of DTE moiety significantly decreased, as well as the triplet excited state energy level. As a result, the cascade photophysical processes involved in TTA upconversion were modulated. First, the S_1 state energy level of the DTE-c moiety decreased to 2.14 eV, which is lower than DPA moiety

(2.98 eV), thus FRET with DPA moiety as singlet energy donor and DTE-c moiety as energy acceptor was activated, the fluorescence of the DPA moiety was quenched (Figure 8a). Second, intermolecular triplet state energy from **Ir-1** to **DTE-c** is also activated, because the **DTE-c** moiety is with much lower triplet state energy level (0.96 eV). Moreover, the intramolecular triplet state energy transfer in DD-o, with the DPA moiety as the triplet energy donor and the DTE-c moiety as the triplet state energy acceptor, is also activated. Third, the CTS energy level of **DD-c** is 2.79 eV (toluene), which is lower than the S_1 state of **DPA**, thus the fluorescence of **DPA** was quenched (Scheme 3b). Based on these analysis, the TTA upconversion will be reduced with **DD-c** as the triplet state acceptor. The photoswitching is reversible, thus the photophysical processes, as well as the TTA upconversion, can be photoswitched.

■ CONCLUSIONS

In summary, a photoswitchable triplet energy acceptor/fluorescent emitter, herein exemplified with a triad based on 9,10-diphenylanthracene (DPA) and dithienylethene (DTE), was developed for the first time for photoswitching of triplet-triplet-annihilation (TTA) upconversion. The triad was prepared by covalently linking DPA and DTE moieties by Click reaction. The fluorescence of the DPA moiety in the triad, as well as the energy level and the confinement of the triplet state of the triad, is able to be photoswitched via the reversible photocyclization and photoreversion of the DTE moiety, as a result the TTA upconversion can be photoswitched ON and OFF. The photophysical processes involved in the photochromism of the triad and the photoswitched TTA upconversion were studied with steady state UV–vis absorption and fluorescence emission spectroscopies, nanosecond transient absorption spectroscopy, electrochemical characterization, and DFT/TDDFT calculations. We concluded that *three* different mechanisms are responsible for the photoswitching of the TTA upconversion with the triad as the triplet acceptor, i.e. the photoactivated fluorescence-resonance-energy-transfer (FRET) in the triad, with DPA as energy donor and the closed form of DTE as energy acceptor; the *intramolecular* electron transfer in the triad, as well as the photoactivated *intermolecular* triplet energy transfer from the Ir(III) complex triplet photosensitizer to the DTE-c moiety. Previously the photoswitching of TTA upconversion was accomplished with only one mechanism, i.e. intermolecular or intramolecular triplet energy transfer. These studies will be useful for designing of photocontrollable TTA upconversion and the application of this kind of upconversion in luminescent bioimaging materials, molecular logic gates, as well as super-resolution fluorescence microscope.

■ EXPERIMENTAL SECTION

Materials and Equipment. All the chemicals are analytically pure and were used as received. Solvents were dried and distilled prior to use. ^{1}H and ^{13}C NMR spectra were recorded on a Bruker 400/500 MHz spectrophotometer ($CDCl_3$ as solvent, TMS as standard for which $\delta = 0.00$ ppm). High resolution mass spectra (HRMS) were determined with ESI-Q-TOF MS spectrometer. Fluorescence spectra were recorded with a RF-5301PC spectrofluorometer (Shimadzu, Japan). Fluorescence lifetimes were measured with OB920 luminescence lifetime spectrometer (Edinburgh, UK). Absorption spectra were recorded on 8453A UV–vis spectrophotometer (Agilent, USA). For synthesis of compounds **1**, **2** and **3**, see the Supporting Information.

Synthesis and Characterization.

Synthesis of the compound **4**. A mixture of compound **3** (200 mg, 0.578 mmol), 1,2-dibromoethane (543 mg, 2.89 mmol), anhydrous K_2CO_3 (159.5 mg, 1.156 mmol) and tetrabutylammonium bromide (TBAB. 3 mg, 9 mmol) was dissolved in dry acetone (15 mL), then the solution was refluxed for 3 days. After completion of the reaction, the solid was filtered, and the solution was evaporated under reduced pressure. Purification of the crude product by column chromatography (silica gel, Petroleum ether/ CH_2Cl_2 = 1: 1) afforded the product as a white solid (130.9 mg). Yield: 50%. mp 224–225 °C. ^{1}H NMR (500 MHz, $CDCl_3$): δ 7.75–7.69 (m, 4H), 7.63–7.54 (m, 3H), 7.50 (d, 2H, *J* = 10.0 Hz), 7.43 (d, 2H, *J* = 10.0 Hz), 7.36–7.31 (m, 4H), 7.16 (d, 2H, *J* = 5.0 Hz), 4.48 (t, 2H, *J* = 5.0 Hz), 3.78 (t, 2H, *J* = 5.0 Hz). MALDI-HRMS: calcd ($[C_{28}H_{21}BrO]^+$), *m/z* = 452.0776, found *m/z* = 452.0775.

*Synthesis of the compound **5**.* Compound **4** (90.6 mg, 0.2 mmol) and NaN_3 (65 mg, 1.0 mmol) were dissolved in DMF (5.0 mL), then the reaction mixture was heated at 100 °C for 1 h. The solution was cooled to r.t. and water (15 mL) was added. The solid was filtered and washed with water for several times. Purification of the product by column chromatography (silica gel, Petroleum ether/ CH_2Cl_2 = 1: 1) afforded the product as a white solid (57.7 mg. 69.5%). mp 202–204 °C. ^{1}H NMR (500 MHz, $CDCl_3$): δ 7.74–7.72 (m, 2H), 7.70–7.68 (m, 2H), 7.62–7.59 (m, 2H), 7.56–7.55 (m, 1H), 7.49–7.47 (m, 2H), 7.42–7.40 (m, 2H,), 7.34–7.31 (m, 4H), 7.18–7.15 (m, 2H), 4.33 (t, 2H, *J* = 5.0 Hz), 3.72 (t, 2H, *J* = 5.0 Hz). MALDI-HRMS: calcd ($[C_{28}H_{21}N_3O]^+$), *m/z* = 415.1685, found *m/z* = 415.1693.

*Synthesis of compound **6**.* A mixture of compound **5** (25 mg, 0.06 mmol) and phenylacetylene (12.3 mg, 0.12 mmol) were dissolved in deaerated $CHCl_3$/ethanol/water (12/1/1, v/v, 14 mL). Triethylamine (3 drops) was added. Then $CuSO_4{\cdot}5H_2O$ (3.0 mg, 0.01 mmol) and sodium ascorbate (2.0 mg, 0.010 mmol) were added. The reaction mixture was stirred at RT for 24 h. After completion of the reaction, water (20 mL) was added, and mixture was extracted with dichloromethane (3×30 mL) and the solution is dried over anhydrous Na_2SO_4. After removal of the solvent under reduced pressure, the mixture was purified by column chromatography (silica gel, CH_2Cl_2) to give white solid. Yield: 21.1 mg (71.0 %). mp > 250 °C. ^{1}H NMR (400 MHz,

$CDCl_3$): δ 8.08 (s, 1H), 7.91–7.88 (m, 2H), 7.70–7.66 (m, 4H), 7.62–7.54 (m, 3H), 7.48–7.44 (m, 4H), 7.42–7.36 (m, 3H), 7.34–7.29 (m, 4H), 7.15–7.12 (m, 2H), 4.94 (t, 2H, J = 4.0 Hz), 4.58–4.55 (t, 2H, J = 4.0 Hz). MALDI-HRMS: calcd ($[C_{36}H_{27}N_3O]^+$), m/z = 517.2154, found m/z = 517.2181.

*Synthesis of the **DD-o***. A mixture of dithienylethene derivative (**DTE-o**, 15.0 mg, 0.036 mmol), and compound **5** (31.4 mg, 0.076 mmol) were dissolved in deaerated $CHCl_3$/ethanol/water (12/1/1, v/v, 14 mL) and triethylamine (3 drops). Then $CuSO_4{\cdot}5H_2O$ (0.01 mmol, 3 mg) and sodium ascorbate (0.010 mmol, 2 mg) were added. The reaction mixture was stirred at RT for 24 h. After completion of the reaction, water (20 mL) was added, and mixture was extracted with dichloromethane (3×30 mL). The organic layers were dried over anhydrous Na_2SO_4. After removal of the solvent under reduced pressure, the mixture was purified by column chromatography (silica gel, CH_2Cl_2) to give gray solid. Yield: 25.1 mg (56.0 %). mp > 250 °C. ^{1}H NMR (400 MHz, $CDCl_3$): δ 7.98 (s, 2H), 7.69–7.66 (m, 7H), 7.60–7.54 (m, 7H), 7.47–7.45 (m, 4H), 7.41– 7.39 (m, 6H), 7.33–7.30 (m, 8H), 7.14 (d, 4H, J = 12.0 Hz), 4.89 (t, 4H, J = 4.0 Hz), 4.55 (t, 4H, J = 4.0 Hz), 1.99 (s, 6H). ^{13}C NMR (100 MHz, $CDCl_3$) : δ = 157.23, 142.14, 141.74, 139.02, 137.18, 136.34, 132.64, 131.29, 130.12, 129.89, 128.42, 127.03, 126.82, 125.04, 120.45, 114.53, 66.49, 50.16, 22.70, 14.59, 14.13. MALDI-HRMS: calcd ($[C_{75}H_{52}N_6O_2F_6S_2]^+$), m/z = 1246.3497, found m/z = 1246.3418.

Cyclic Voltammetry Curves. The cyclic voltammetry curves were recorded by CH instruments (CH instruments, Inc. Shanghai, China). In N_2 saturated CH_3CN containing a 0.10 M Bu_4NPF_6 as supporting electrolyte; counter electrode is Pt electrode; working electrode is glassy carbon electrode; Ag/$AgNO_3$ couple as the reference electrode. c [Ag^+] = 0.1 M. 1.0 mM compounds in CH_3CN, 20 °C. Scan rates: 50 mV/s. Ferrocene (Fc) was used as internal reference.

Nanosecond Transient Absorption Spectra. The nanosecond time-resolved transient absorption spectra were recorded on LP920 laser flash photolysis spectrometer (Edinburgh Instruments, UK). The signal was buffered on a Tektronix TDS 3012B oscilloscope. All samples in flash photolysis experiments were deaerated with argon for ca. 15 min before measurement.

DFT Calculations. The ground state structures of compounds were optimized using DFT with B3LYP functional and 6–31G(d) basis set. The excited-state related calculations (UV−vis absorptions) were carried out with the time-dependent DFT (TDDFT) with the optimized structure of the ground state (DFT/6–31G(d)). The emission of the fluorophores were calculated based on the TDDFT optimized S_1 excited state geometry. There are no imaginary frequencies in frequency analysis of all calculated structures. All of these calculations were performed with Gaussian 09W.[69]

Triplet-triplet annihilation upconversion. The excitation source for the upconversion is diode pumped solid state (DPSS) continuous laser (445 nm). The power of the laser beam was measured with VLP-2000 pyroelectric laser power meter and the diameter of the 445 nm laser spot is ca. 3 mm. The mixed solution of the Ir(III) complex (triplet photosensitizers) and DPA derivative was degassed with N_2 for about 15 min. RF5301PC spectrofluorometer (Shimadzu, Japan) was applied in the upconverted fluorescence measurement. A small black box behind the fluorescent cuvette to damp the laser beam to repress the scattered laser.

Eq. 5 was used to calculate the upconversion quantum yields, Φ_{UC}, A_{sam}, I_{sam} and η_{sam} represents the quantum yield, absorbance, integrated photoluminescence intensity and the refractive index of the solvents (where the subscript “std” is for the standard used in the measurement and the “sam” is for the samples measured). The equation is multiplied by a factor of 2 so as to set the maximum quantum yield to unity.

$$\Phi_{\mathrm{UC}} = 2\Phi_{\mathrm{std}}\left(\frac{A_{\mathrm{std}}}{A_{\mathrm{sam}}}\right)\left(\frac{I_{\mathrm{sam}}}{I_{\mathrm{std}}}\right)\left(\frac{\eta_{\mathrm{sam}}}{\eta_{\mathrm{std}}}\right)^2 \qquad \text{Eq. 5}$$

AKNOWLEDGEMENT

We thank the NSFC (20972024, 21273028, 21421005 and 21473020), the Royal Society (UK) and NSFC (China-UK Cost-Share Science Networks, 21011130154), and Ministry of Education (SRFDP-20120041130005), Program for Changjiang Scholars and Innovative Research Team in University [IRT_13R06], the Fundamental Research Funds for the Central Universities (DUT14ZD226) and Dalian University of Technology (DUT2013TB07) for financial support.

REFERENCES

(1) Liu, J.; Liu, Y.; Liu, Q.; Li, C.; Sun, L.; Li, F. Iridium(III) Complex-Coated Nanosystem for Ratiometric Upconversion Luminescence Bioimaging of Cyanide Anions. *J. Am. Chem. Soc.* **2011,** *133*, 15276–15279.

(2) Liu, Q.; Yang, T.; Feng, W.; Li, F. Blue-Emissive Upconversion Nanoparticles for Low-Power-Excited Bioimaging in Vivo. *J. Am. Chem. Soc.* **2012**, *134* (11), 5390–5397.

(3) Lissau, J. S.; Gardner, J. M.; Morandeira, A. Photon Upconversion on Dye-Sensitized Nanostructured ZrO_2 Films. *J. Phys. Chem. C.* **2011**, *115*, 23226–23232.

(4) Schulze, T. F.; Czolk, J.; Cheng, Y.-Y.; Fückel, B.; MacQueen, R. W.; Khoury, T.; Crossley, M. J.; Stannowski, B.; Lips, K.; Lemmer, U.; et al. Efficiency Enhancement of Organic and Thin-Film Silicon Solar Cells with Photochemical Upconversion. *J. Phys. Chem. C.* **2012**, *116*, 22794–22801.

(5) Nattestad, A.; Cheng, Y. Y.; MacQueen, R. W.; Schulze, T. F.; Thompson, F. W.; Mozer, A. J.; Fückel, B.; Khoury, T.; Crossley, M. J.; Lips, K.; et al. Dye-Sensitized Solar Cell with

Integrated Triplet–Triplet Annihilation Upconversion System. *J. Phys. Chem. Lett.* **2013**, *4*, 2073–2078.

(6) Khnayzer, R. S.; Blumhoff, J.; Harrington, J. A.; Haefele, A.; Deng, F.; Castellano, F. N. Upconversion-powered photoelectrochemistry. *Chem. Commun.* **2012**, *48*, 209–211.

(7) Singh-Rachford, T. N.; Castellano, F. N. Photon Upconversion Based on Sensitized Triplet–triplet Annihilation. *Coord. Chem. Rev.* **2010**, *254*, 2560–2573.

(8) Zhao, J.; Ji, S.; Guo, H. Triplet-triplet Annihilation Based Upconversion: From Triplet Sensitizers and Triplet Acceptors to Upconversion Quantum Yields. *RSC Adv.* **2011**, *1*, 937–950.

(9) Ceroni, P. Energy Up-Conversion by Low-Power Excitation: New Applications of an Old Concept. *Chem. Eur. J.* **2011**, *17*, 9560–9564.

(10) Simon, Y. C.; Weder, C. Low-power Photon Upconversion through Triplet-triplet Annihilation in Polymers. *J. Mater. Chem.* **2012**, *22*, 20817–20830.

(11) Irie, M. Diarylethenes for Memories and Switches. *Chem. Rev.* **2000**, *100*, 1685–1716.

(12) Léaustic, A.; Anxolabéhère-Mallart, E.; Maurel, F.; Midelton, S.; Guillot, R.; Métivier, R.; Nakatani, K.; Yu, P. Photochromic and Reductive Electrochemical Switching of a Dithiazolylethene with Large Redox Modulation. *Chem. Eur. J.* **2011**, *17*, 2246–2255.

(13) Spangenberg, A.; Metivier, R.; Yasukuni, R.; Shibata, K.; Brosseau, A.; Grand, J.; Aubard, J.; Yu, P.; Asahi, T.; Nakatani, K. Photoswitchable Interactions between Photochromic Organic Diarylethene and Surface Plasmon Resonance of Gold Nanoparticles in Hybrid Thin Films. *Phys. Chem. Chem. Phys.* **2013**, *15*, 9670–9678.

(14) Myles, A. J.; Wigglesworth, T. J.; Branda, N. R. A Multi-Addressable Photochromic 1,2-Dithienylcyclopentene-Phenoxynaphthacenequinone Hybrid. *Adv. Mater.* **2003**, *15*, 745–748.

(15) Liu, K.; Wen, Y.; Shi, T.; Li, Y.; Li, F.; Zhao, Y.-l.; Huang, C.; Yi, T. DNA Gated Photochromism and Fluorescent Switch in a Thiazole Orange Modified Diarylethene. *Chem. Commun.* **2014**, *50*, 9141−9144.

(16) Boixel, J.; Guerchais, V.; Le Bozec, H.; Jacquemin, D.; Amar, A.; Boucekkine, A.; Colombo, A.; Dragonetti, C.; Marinotto, D.; Roberto, D.; et al. Second-Order NLO Switches from Molecules to Polymer Films Based on Photochromic Cyclometalated Platinum(II) Complexes. *J. Am. Chem. Soc.* **2014**, *136*, 5367−5375.

(17) Zou, Y.; Yi, T.; Xiao, S.; Li, F.; Li, C.; Gao, X.; Wu, J.; Yu, M.; Huang, C. Amphiphilic Diarylethene as a Photoswitchable Probe for Imaging Living Cells. *J. Am. Chem. Soc.* **2008**, *130*, 15750−15751.

(18) Roberts, M. N.; Carling, C.-J.; Nagle, J. K.; Branda, N. R.; Wolf, M. O. Successful Bifunctional Photoswitching and Electronic Communication of Two Platinum(II) Acetylide Bridged Dithienylethenes. *J. Am. Chem. Soc.* **2009**, *131*, 16644−16645.

(19) Ishibashi, Y.; Fujiwara, M.; Umesato, T.; Saito, H.; Kobatake, S.; Irie, M.; Miyasaka, H. Cyclization Reaction Dynamics of a Photochromic Diarylethene Derivative as Revealed by Femtosecond to Microsecond Time-Resolved Spectroscopy. *J. Phys. Chem. C.* **2011**, *115*, 4265−4272.

(20) Zhang, J.; Riskin, M.; Tel-Vered, R.; Tian, H.; Willner, I. Optically Activated Uptake and Release of Cu^{2+} or Ag^{+} Ions by or from a Photoisomerizable Monolayer-Modified Electrode. *Langmuir*. **2010**, *27*, 1380−1386.

(21) Wen, H.-M.; Li, B.; Wang, J.-Y.; Shi, L.-X.; Chen, C.-N.; Chen, Z.-N. Multistate Photochromism in a Ruthenium Complex with Dithienylethene–Acetylide. *Organometallics* **2013**, *32*, 1759−1765.

(22) Li, Z.; Zhang, C.; Ren, Y.; Yin, J.; Liu, S. H. Amide- and Urea-Functionalized Dithienylethene: Synthesis, Photochromism, and Binding with Halide Anions. *Org. Lett.* **2011**, *13*, 6022−6025.

(23) Yasukuni, R.; Boubekri, R.; Grand, J.; Félidj, N.; Maurel, F.; Perrier, A.; Métivier, R.; Nakatani, K.; Yu, P.; Aubard, J. Specific and Nondestructive Detection of Different Diarylethene Isomers by NIR-SERS. *J. Phys. Chem. C.* **2012**, *116*, 16063−16069.

(24) Szalóki, G.; Sevez, G.; Berthet, J.; Pozzo, J.-L.; Delbaere, S. A Simple Molecule-Based Octastate Switch. *J. Am. Chem. Soc.* **2014,** *136*, 13510−13513.

(25) Li, B.; Wen, H.-M.; Wang, J.-Y.; Shi, L.-X.; Chen, Z.-N. Modulating Stepwise Photochromism in Platinum(II) Complexes with Dual Dithienylethene–Acetylides by a Progressive Red Shift of Ring-Closure Absorption. *Inorg. Chem.* **2013**, *52*, 12511−12520.

(26) Li, B.; Wang, J.-Y.; Wen, H.-M.; Shi, L.-X.; Chen, Z.-N. Redox-Modulated Stepwise Photochromism in a Ruthenium Complex with Dual Dithienylethene-Acetylides. *J. Am. Chem. Soc.* **2012**, *134*, 16059−16067.

(27) Boyer, J.-C.; Carling, C.-J.; Gates, B. D.; Branda, N. R. Two-Way Photoswitching Using One Type of Near-Infrared Light, Upconverting Nanoparticles, and Changing Only the Light Intensity. *J. Am. Chem. Soc.* **2010**, *132*, 15766−15772.

(28) Lin, Y.; Yuan, J.; Hu, M.; Cheng, J.; Yin, J.; Jin, S.; Liu, S. H. Syntheses and Properties of Binuclear Ruthenium Vinyl Complexes with Dithienylethene Units as Multifunction Switches. *Organometallics.* **2009**, *28*, 6402−6409.

(29) Hu, F.; Huang, J.; Cao, M.; Chen, Z.; Yang, Y.-W.; Liu, S. H.; Yin, J. Dithienylethene-based Rotaxanes: Synthesis, Characterization and Properties. *Org. Biomol. Chem.* **2014**, *12*, 7712−7720.

(30) Pu, S.; Tong, Z.; Liu, G.; Wang, R. Multi-addressable Molecular Switches Based on a New Diarylethene Salicylal Schiff Base Derivative. *J. Mater. Chem. C.* **2013**, *1*, 4726–4739.

(31) Deniz, E.; Battal, M.; Cusido, J.; Sortino, S.; Raymo, F. M. Insights into the Isomerization of Photochromic Oxazines from the Excitation Dynamics of BODIPY-Oxazine Dyads. *Phys. Chem. Chem. Phys.* **2012**, *14*, 10300−10307.

(32) Golovkova, T. A.; Kozlov, D. V.; Neckers, D. C. Synthesis and Properties of Novel Fluorescent Switches. *J. Org. Chem.* **2005**, *70*, 5545−5549.

(33) Kong, L.; Wong, H.-L.; Tam, A. Y.-Y.; Lam, W. H.; Wu, L.; Yam, V. W.-W. Synthesis, Characterization, and Photophysical Properties of Bodipy-Spirooxazine and -Spiropyran Conjugates: Modulation of Fluorescence Resonance Energy Transfer Behavior via Acidochromic and Photochromic Switching. *ACS Appl. Mater. Interfaces.* **2014**, *6*, 1550−1562.

(34) Xie, N.; Chen, Y. Combination of Fluorescent Switch and Electrochemical Switch Based on a Photochromic Diarylethene. *New J. Chem.* **2006**, *30*, 1595−1598.

(35) Tomasulo, M.; Deniz, E.; Alvarado, R. J.; Raymo, F. M. Photoswitchable Fluorescent Assemblies Based on Hydrophilic BODIPY−Spiropyran Conjugates. *J. Phys. Chem. C.* **2008**, *112*, 8038−8045.

(36) Berberich, M.; Krause, A.-M.; Orlandi, M.; Scandola, F.; Würthner, F. Toward Fluorescent Memories with Nondestructive Readout: Photoswitching of Fluorescence by Intramolecular Electron Transfer in a Diaryl Ethene-Perylene Bisimide Photochromic System. *Angew. Chem. Int. Ed.* **2008**, *47*, 6616–6619.

(37) Fukaminato, T.; Tanaka, M.; Doi, T.; Tamaoki, N.; Katayama, T.; Mallick, A.; Ishibashi, Y.; Miyasaka, H.; Irie, M. Fluorescence Photoswitching of a Diarylethene-Perylenebisimide Dyad Based on Intramolecular Electron Transfer. *Photochem. Photobiol. Sci.* **2010**, *9*, 181−187.

(38) Fukaminato, T.; Doi, T.; Tamaoki, N.; Okuno, K.; Ishibashi, Y.; Miyasaka, H.; Irie, M. Single-Molecule Fluorescence Photoswitching of a Diarylethene−Perylenebisimide Dyad: Non-destructive Fluorescence Readout. *J. Am. Chem. Soc.* **2011**, *133*, 4984–4990.

(39) Pu, S.; Jiang, D.; Liu, W.; Liu, G.; Cui, S. Multi-addressable Molecular Switches based on Photochromic Diarylethenes Bearing a Rhodamine Unit. *J. Mater. Chem.* **2012**, *22*, 3517–3526.

(40) Yagai, S.; Ishiwatari, K.; Lin, X.; Karatsu, T.; Kitamura, A.; Uemura, S. Rational Design of Photoresponsive Supramolecular Assemblies Based on Diarylethene. *Chem. Eur. J.* **2013**, *19*, 6971–6975.

(41) He, B.; Wenger, O. S. Ruthenium-Phenothiazine Electron Transfer Dyad with a Photoswitchable Dithienylethene Bridge: Flash-Quench Studies with Methylviologen. *Inorg. Chem.* **2012**, *51*, 4335–4342.

(42) Frey, J.; Kodis, G.; Straight, S. D.; Moore, T. A.; Moore, A. L.; Gust, D. Photonic Modulation of Electron Transfer with Switchable Phase Inversion. *J. Phys. Chem. A.* **2012**, *117*, 607–615.

(43) Ordronneau, L.; Boixel, J.; Aubert, V.; Vidal, M. S.; Moya, S.; Aguirre, P.; Toupet, L.; Williams, J. A. G.; Le Bozec, H.; Guerchais, V. New Ffluorescent Bis-dithienylethene (DTE)-Based Bipyridines as Reverse Interrupters: Single vs. Double Photochromism. *Org. Biomol. Chem.* **2014**, *12*, 979–992.

(44) Fukaminato, T.; Umemoto, T.; Iwata, Y.; Yokojima, S.; Yoneyama, M.; Nakamura, S.; Irie, M. Photochromism of Diarylethene Single Molecules in Polymer Matrices. *J. Am. Chem. Soc.* **2007**, *129*, 5932–5938.

(45) Sánchez, R. S.; Gras-Charles, R.; Bourdelande, J. L.; Guirado, G.; Hernando, J. Light- and Redox-Controlled Fluorescent Switch Based on a Perylenediimide–Dithienylethene Dyad. *J. Phys. Chem. C.* **2012**, *116*, 7164−7172.

(46) Jukes, R. T. F.; Adamo, V.; Hartl, F.; Belser, P.; De Cola, L. Photochromic Dithienylethene Derivatives Containing Ru(II) or Os(II) Metal Units. Sensitized Photocyclization from a Triplet State. *Inorg. Chem.* **2004**, *43*, 2779–2792.

(47) Ko, C.-C.; Kwok, W.-M.; Yam, V. W.-W.; Phillips, D. L. Triplet MLCT Photosensitization of the Ring-Closing Reaction of Diarylethenes by Design and Synthesis of a Photochromic Rhenium(I) Complex of a Diarylethene-Containing 1,10-Phenanthroline Ligand. *Chem. Eur. J.* **2006**, *12*, 5840−5848.

(48) Indelli, M. T.; Carli, S.; Ghirotti, M.; Chiorboli, C.; Ravaglia, M.; Garavelli, M.; Scandola, F. Triplet Pathways in Diarylethene Photochromism: Photophysical and Computational Study of Dyads Containing Ruthenium(II) Polypyridine and 1,2-Bis(2-methylbenzothiophene-3-yl)maleimide Units. *J. Am. Chem. Soc.* **2008**, *130*, 7286−7299.

(49) Tan, W.; Zhang, Q.; Zhang, J.; Tian, H. Near-Infrared Photochromic Diarylethene Iridium (III) Complex. *Org. Lett.* **2008**, *11*, 161−164.

(50) Cui, X.; Zhao, J.; Zhou, Y.; Ma, J.; Zhao, Y. Reversible Photoswitching of Triplet–Triplet Annihilation Upconversion Using Dithienylethene Photochromic Switches. *J. Am. Chem. Soc.* **2014**, *136*, 9256–9259.

(51) Lee, M. K.; Rai, P.; Williams, J.; Twieg, R. J.; Moerner, W. E. Small-Molecule Labeling of Live Cell Surfaces for Three-Dimensional Super-Resolution Microscopy. *J. Am. Chem. Soc.* **2014**, *136*, 14003−14006.

(52) Li, C.; Gong, W.-L.; Hu, Z.; Aldred, M. P.; Zhang, G.-F.; Chen, T.; Huang, Z.-L.; Zhu, M.-Q. Photoswitchable Aggregation-Induced Emission of a Dithienylethene-Tetraphenylethene Conjugate for Optical Memory and Super-Resolution Imaging. *RSC Adv.* **2013**, *3*, 8967−8972.

(53) Wu, Y.; Xie, Y.; Zhang, Q.; Tian, H.; Zhu, W.; Li, A. D. Q. Quantitative Photoswitching in Bis(dithiazole)ethene Enables Modulation of Light for Encoding Optical Signals. *Angew. Chem. Int. Ed.* **2014**, *53*, 2090−2094.

(54) Ji, S.; Wu, W.; Wu, W.; Guo, H.; Zhao, J. Ruthenium(II) Polyimine Complexes with a Long-Lived ^{3}IL Excited State or a ^{3}MLCT/^{3}IL Equilibrium: Efficient Triplet Sensitizers for Low-Power Upconversion. *Angew. Chem. Int. Ed.* **2011**, *50*, 1626−1629.

(55) Osuka, A.; Fujikane, D.; Shinmori, H.; Kobatake, S.; Irie, M. Synthesis and Photoisomerization of Dithienylethene-Bridged Diporphyrins. *J. Org. Chem.* **2001**, *66*, 3913−3923.

(56) Deniz, E.; Sortino, S.; Raymo, F. M. Fast Fluorescence Photoswitching in a BODIPY−Oxazine Dyad with Excellent Fatigue Resistance. *J. Phys. Chem. Lett.* **2010**, *1*, 1690−1693.

(57) Sun, J.; Wu, W.; Guo, H.; Zhao, J. Visible-Light Harvesting with Cyclometalated Iridium(III) Complexes Having Long-Lived ^{3}IL Excited States and Their Application in Triplet–Triplet-Annihilation Based Upconversion. *Eur. J. Inorg. Chem.* **2011**, 3165−3173.

(58) Whited, M. T.; Djurovich, P. I.; Roberts, S. T.; Durrell, A. C.; Schlenker, C. W.; Bradforth, S. E.; Thompson, M. E. Singlet and Triplet Excitation Management in a Bichromophoric Near-Infrared-Phosphorescent BODIPY-Benzoporphyrin Platinum Complex. *J. Am. Chem. Soc.* **2010**, *133*, 88−96.

(59) El-Khouly, M. E.; Amin, A. N.; Zandler, M. E.; Fukuzumi, S.; D'Souza, F. Near-IR Excitation Transfer and Electron Transfer in a BF_2-Chelated Dipyrromethane–Azadipyrromethane Dyad and Triad. *Chem. Eur. J.* **2012**, *18*, 5239−5247.

(60) Lee, S.; You, Y.; Ohkubo, K.; Fukuzumi, S.; Nam, W. Highly Efficient Cycloreversion of Photochromic Dithienylethene Compounds Using Visible Light-Driven Photoredox Catalysis. *Chem. Sci.* **2014**, *5*, 1463−1474.

(61) Wolf, J.; Eberspächer, I.; Groth, U.; Huhn, T. Synthesis and Photoswitching Studies of OPE-Embedded Difurylperfluorocyclopentenes. *J. Org. Chem.* **2013**, *78*, 8366−8375.

(62) Kim, H. J.; Jang, J. H.; Choi, H.; Lee, T.; Ko, J.; Yoon, M.; Kim, H.-J. Photoregulated Fluorescence Switching in Axially Coordinated Tin(IV) Porphyrinic Dithienylethene. *Inorg. Chem.* **2008**, *47*, 2411−2415.

(63) Lakowicz, J. R. *Principles of Fluorescence Spectroscopy*, Kluwer Academic/Plenum Publishers, New York, 2nd edn, **1999**.

(64) Ordronneau, L.; Nitadori, H.; Ledoux, I.; Singh, A.; Williams, J. A. G.; Akita, M.; Guerchais, V.; Le Bozec, H. Photochromic Metal Complexes: Photoregulation of Both the Nonlinear Optical and Luminescent Properties. *Inorg. Chem.* **2012**, *51*, 5627−5636.

(65) Roberts, M. N.; Nagle, J. K.; Finden, J. G.; Branda, N. R.; Wolf, M. O. Linker-Dependent Metal-Sensitized Photoswitching of Dithienylethenes. *Inorg. Chem.* **2008**, *48*, 19−21.

(66) Zhang, C.; Zhao, J.; Wu, S.; Wang, Z.; Wu, W.; Ma, J.; Guo, S.; Huang, L. Intramolecular RET Enhanced Visible Light-Absorbing Bodipy Organic Triplet Photosensitizers and Application in Photooxidation and Triplet–Triplet Annihilation Upconversion. *J. Am. Chem. Soc.* **2013**, *135*, 10566−10578.

(67) Hou, L.; Zhang, X.; Pijper, T. C.; Browne, W. R.; Feringa, B. L. Reversible Photochemical Control of Singlet Oxygen Generation Using Diarylethene Photochromic Switches. *J. Am. Chem. Soc.* **2014**, *136*, 910–913.

(68) Chen, H.-C.; Hung, C.-Y.; Wang, K.-H.; Chen, H.-L.; Fann, W. S.; Chien, F.-C.; Chen, P.; Chow, T. J.; Hsu, C.-P.; Sun, S.-S. White-light Emission from an Upconverted Emission with an Organic Triplet Sensitizer. *Chem. Commun.* **2009**, 4064–4066.

(69) Frisch, M. J.; Trucks, G. W.; Schlegel, H. B.; Scuseria, G. E.; Robb, M. A.; Cheeseman, J. R.; Scalmani, G.; Barone, V.; Mennucci, B.; Petersson, G. A.; et al., *Gaussian 09*, Revision 01, Gaussian Inc., Wallingford, CT, 2009.

Table of Contents